J Am Soc Nephrol 15: 286–298, 2004

Exogenous PDGF-D Is a Potent Mesangial Cell Mitogen and Causes a Severe Mesangial Proliferative Glomerulopathy

KELLY L. HUDKINS,* DEBRA G. GILBERTSON,† MATTHEW CARLING,* SEKIKO TANEDA,* STEVEN D. HUGHES,† MATTHEW S. HOLDREN,† THOMAS E. PALMER,† STAVROS TOPOUZIS,† AARON C. HARAN,† ANDREW L. FELDHAUS,† and CHARLES E. ALPERS*

**University of Washington, Seattle, Washington; and †Zymogenetics, Inc., Seattle, Washington*

Abstract. The PDGF family consists of at least four members, PDGF-A, -B, -C, and -D. All of the PDGF isoforms bind and signal through two known receptors, PDGF receptor-α and PDGF receptor-β, which are constitutively expressed in the kidney and are upregulated in specific diseases. It is well established that PDGF-B plays a pivotal role in the mediation of glomerular mesangial cell proliferation. However, little is known of the roles of the recently discovered PDGF-C and -D in mediating renal injury. In this study, adenovirus constructs encoding PDGF-B, -C, and -D were injected into mice. Mice with high circulating levels of PDGF-D developed a severe mesangial proliferative glomerulopathy, characterized by enlarged glomeruli and a striking increase in glomerular cellularity. The PDGF-B–overexpressing mice had a milder proliferative glomerulopathy, whereas the mice overexpressing PDGF-C and those that received adenovirus alone showed no measurable response. Mitogenicity of PDGF-D and -B for mesangial cells was confirmed *in vitro*. These findings emphasize the importance of engagement of PDGF receptor-β in transducing mesangial cell proliferation and demonstrate that PDGF-D is a major mediator of mesangial cell proliferation. Finally, this approach has resulted in a unique and potentially valuable model of mesangial proliferative glomerulopathy and its resolution.

Proliferation of mesangial cells and accumulation of extracellular matrix characterize a wide variety of progressive renal diseases. The best characterized mediators of mesangial cell proliferation are the members of the PDGF family of growth factors (1–5).

The PDGF family consists of at least four members, PDGF-A, -B, -C, and -D. Of these, PDGF-A and -B have been studied extensively in the context of renal disease, but little is known of the recently discovered family members PDGF-C and -D. The original members of the PDGF family are processed intracellularly and secreted as disulfide bonded homo- or heterodimers (PDGF-AA, -BB, and -AB). In contrast, PDGF-C and -D both have a unique two-domain structure, with an amino terminal CUB domain and a C-terminal growth factor domain (GFD) (6–8), and are secreted in a latent full-length form (designated PDGF-C and -D). Both of these peptides require extracellular proteolytic cleavage to release the biologically active GFD (designated PDGF-CC and -DD). The GFD of PDGF-C and -D share significant homology with one another (approximately 50%) and with the previously described PDGF (20 to 23%) (7, 8).

There are two known tyrosine kinase receptors for PDGF, PDGF receptor-α (PDGFR-α) and PDGF receptor-β (PDGFR-β). These receptors are bivalent and can exist in any of three possible combinations, PDGF receptor-α/α, -β/β, or -α/β. The receptor subunits require PDGF-mediated dimerization for ligand binding and signaling (9). The accepted paradigm for the last two decades has been that PDGF-A binds and signals only through PDGFR-$\alpha\alpha$, and PDGF-B can bind both PDGFR-$\beta\beta$ and PDGFR-α/β (10–12). It has now been shown that activated PDGF-CC can bind to both PDGFR-α and -α/β (6, 8), whereas PDGF-DD is the only known PDGFR-β–specific ligand (7).

Increased expression of PDGF-A and -B and PDGF receptors has been shown in a wide variety of human and experimental renal diseases (13). It is well established that PDGF-B, signaling through PDGFR-β, plays a pivotal role in the mediation of glomerular mesangial cell proliferation and interstitial fibrosis (3, 14–18). Recent studies have shown that PDGF-C is expressed constitutively in rat and human kidney and that it is upregulated in mesangial cells, visceral epithelial cells, and interstitial cells in injury states (19, 20). PDGF-C is a mitogen for cells of mesenchymal origin *in vitro*, including rat mesangial cells (19). Although it was shown recently that PDGF-D is expressed constitutively in human kidney by visceral epithelial cells and vascular smooth muscle cells, no information is available on its potential function in the kidney (21). On the basis of its known binding properties to PDGFR-β, we sought to investigate whether PDGF-D could mediate mesangial pro-

Received May 19, 2003. Accepted October 31, 2003.
Dr. Roger Wiggins served as Guest Editor and supervised the review and final disposition of this manuscript.
Correspondence to Dr. Charles E. Alpers, University of Washington, Department of Pathology, Box 357470, Seattle, WA 98195. Phone: 206-598-6409; Fax: 206-543-3644; E-mail: calp@u.washington.edu

1046-6673/1502-0286
Journal of the American Society of Nephrology

DOI: 10.1097/01.ASN.0000108522.79652.63

liferative injury. Using adenovirus constructs containing the coding regions of PDGF-B, -C, and -D to produce elevated systemic levels of these peptides in mice, we were surprised to find that PDGF-D might be the most potent stimulus for murine mesangial cell proliferation identified to date. The effects of PDGF-D extended beyond mesangial cell proliferation and resulted in a mesangial proliferative glomerulonephritis characterized by a large glomerular macrophage influx, collagen IV–positive matrix accumulation, and activation of mesangial cells as demonstrated by increased α-smooth muscle actin (α-SMA) expression. Accordingly, we demonstrate an important biologic activity in the glomerulus for PDGF-D, localize its constitutive pattern of expression in normal murine kidney, which differs from its pattern of expression in humans, and characterize a murine model of mesangial proliferative glomerulonephritis resulting from systemic overexpression of this peptide.

Materials and Methods

Adenoviral Constructs

Adenoviral constructs were generated as previously published (6). Briefly, the protein coding regions of PDGF-B, -C, and -D were cloned into a modified pAdTrack-CMV construct containing the green fluorescence protein (GFP) marker gene in which the CMV promoter was replaced with the SV40 promoter and the SV40 polyadenylation signal was replaced with the human growth hormone polyadenylation signal site. Recombinant adenovirus constructs were then propagated in 293A cells (Quantum Biotechnologies [Qbiogene], Carlsbad, CA) and purified on cesium chloride gradients. Viral particle numbers were determined by spectrophotometry, and infectious particle numbers were determined by TCID 50 assay (Quantum Biotechnologies).

Animal Studies

In a pilot study, female C57Bl/6 mice were given a single intravenous injection of 1.0×10^{11} particles of adenovirus-GFP (Ad) alone ($n = 8$), Ad-PDGF-B ($n = 8$), Ad-PDGF-C ($n = 8$), or Ad-PDGF-D ($n = 8$) or left untreated ($n = 9$). The mice were killed at 3 wk after injection. At necropsy, kidneys were collected in neutral-buffered formalin, processed, and embedded according to standard protocols. Serum was collected at necropsy for determination of serum levels of PDGF by ELISA assay.

A time-course study involved the serial killing of mice at 2-wk intervals after injection with the adenovirus constructs as described above in the pilot study. At each time point (2, 4, 6, and 8 wk), four mice in the Ad, Ad-PDGF-B, Ad-PDGF-C, and Ad-PDGF-D groups and two untreated control mice were killed. Kidney tissue was collected in neutral-buffered formalin and methyl Carnoy's solution (60% methanol, 30% acetic acid, and 10% chloroform), then processed and embedded in paraffin by standard histologic methods. Small pieces of kidney tissue were snap-frozen for use either for RNA isolation or for immunofluorescence studies. Tissue was also collected in half-strength Karnovsky's fixative for electron microscopic examination. Blood was collected for routine renal function analysis and measurements of circulating PDGF levels. For routine pathologic examination, the formalin-fixed tissue was stained with hematoxylin and eosin (H&E), the periodic acid-Schiff reagent, and modified silver methenamine.

Laboratory Data

Serum creatinine and blood urea nitrogen levels were measured using a standard clinical chemistry analyzer (Hitachi AJTICHI 747; Roche, Indianapolis, IN). ELISA were developed to detect and quantify PDGF-CC and -DD, which used monoclonal anti-PDGF antibodies. The antibodies were tested for cross-reactivity to other PDGF isoforms before their use in the ELISA assay. The mAb against PDGF-CC reacted only with the GFD of PDGF-C, whereas the antibody against PDGF-DD recognized both the full-length and the GFD of PDGF-D. The primary mAb was coated onto 96-well microtiter plates at 1 μg/ml in 0.1 mol/L Na_2HCO_3 (pH 9.6) and incubated overnight at 4°C. The plates were washed with PBS containing 0.05% Tween 20, then blocked with PBS containing 0.1% BSA and 0.05% Tween 20 for 2 h at 37°C. Test samples of known PDGF standards were diluted in blocking buffer and incubated for 1 h at 37°C. For PDGF-CC and -DD ELISA, plates were washed and incubated with a ligand-specific biotinylated secondary mAb at 0.5 μg/ml to wells for 1 h at 37°C. The plates were washed, then incubated with streptavidin conjugated to horseradish peroxidase (Pierce, Rockford, IL) at 0.5 μg/ml diluted in blocking buffer. For PDGF-BB ELISA, a well-characterized rabbit anti–B chain polyclonal antibody was added at 1 μg/ml to wells for 1 h at 37°C. The plates were washed, then incubated with goat anti-rabbit IgG conjugated to horseradish peroxidase (Biosource, Camarillo, CA). After a wash, all plates were incubated with OPD substrate (12.5 ml 0.1 mol/L Na citrate [pH 5.0], 5 mg *o*-phenylenediamine [Pierce], 10 μl of 30% H_2O_2) for 10 min at ambient temperature. The reaction was stopped by the addition of 1 N H_2SO_4, and the plates were read at an absorbance of 490 nm in a SpectraMax 340 ELISA plate reader (Molecular Devices, Sunnyvale, CA).

Immunohistochemistry

The protocol used for immunohistochemistry has previously been described in detail (22–24). Antibodies used in this study are listed in Table 1.

Sections of either formalin-fixed or methyl Carnoy's–fixed, paraffin-embedded tissue were used for single-label immunohistochemistry for most reagents, as noted in Table 1. The CD31 antibody was used on frozen tissue sections postfixed in acetone.

Double immunohistochemistry was performed on methyl Carnoy's–fixed tissue sections using antibodies to Ki-67, α-SMA, and Mac-2. The slides were first immunostained with the Ki-67 antibody, using the Animal Research Kit (Dako, Carpinteria, CA) according to the manufacturer's instructions and diaminobenzidine without nickel enhancement, resulting in a brown reaction product. The slides were then incubated sequentially with either rat anti–Mac-2 (Cedarlane, Hornby, Ontario, Canada) or mouse anti–α-SMA (Dako), the appropriate biotinylated secondary antibody (see Table 1), ABC-Elite (Vector, Burlingame, CA), and Vector VIP Substrate to yield a purple reaction product.

TUNEL

To detect DNA fragments characteristic of apoptosis by TUNEL, we used the TdT-FragEL DNA Fragmentation Detection kit (Oncogene Research Products, Boston, MA), as described previously (25).

Morphometric Analysis

Morphometry was performed on H&E- and silver methenamine–stained slides, as well as on slides immunostained for collagen IV accumulations as a principal component of the glomerular matrix by an observer who was blinded to the origin of the sections. From each stained histologic section, 15 consecutive glomerular cross-sections were photographed using an Olympus DP11 digital camera (Olympus

Table 1. Antibodies used for immunohistochemistry

Antibody	Clone	Host	Source	Secondary (Source)	Tissue Fixative	Reference
Mac-2	M3/38	Rat	CedarLane (Hornby, Ontario, Canada)	Bio-anti-rat (Vector)	NBF or MC	(37–39)
CD45, common leukocyte marker	30F11	Rat	Pharmingen (San Diego, CA)	Bio-anti-rat (Vector)	MC	(39)
CD31, endothelial marker	MEC 13.3	Rat	Pharmingen	Bio- anti-rat (Vector)	Acetone (frozen)	(40, 41)
Collagen IV		Goat	Southern Biotechnology (Birmingham, AL)	Bio-anti-goat (Vector)	MC	(26)
α-Smooth muscle actin	1A4	Mouse	Dako (Carpinteria, CA)	Bio-anti-mouse IgG2a (Pharmingen)	MC	(23, 26, 29, 42)
Ki-67	B56	Mouse	Pharmingen	ARK Kit (Dako)	NBF	(43)
PDGF-B (Ab-1)		Rabbit	Oncogene Research (La Jolla, CA)	Bio-anti-rabbit (Vector)	MC	(44)
PDGFR-β (958)		Rabbit	Santa Cruz (Santa Cruz, CA)	Bio-anti-rabbit (Vector)	MC	(45–47)
PDGF-D		Rabbit	ZymoGenetics (Seattle, WA)	Bio-anti-rabbit (Vector)	MC	(21)
T cell	CD3-2	Rat	Pharmingen	Bio-anti- rat (Vector)	MC	(39)
Neutrophil	7/4	Rat	Accurate (Westbury, NY)	Bio-anti-rat (Vector)	MC	(48)
WT-1		Rabbit	Santa Cruz	Bio-anti-rabbit (Vector)	MC	(35, 49)

Bio, biotinylated; ARK, Animal Research Kit; NBF, neutral-buffered formalin; MC, methyl Carnoy's

America, Melville, NY), and the images were imported into the Image-Pro Plus (Media Cybernetics, Silver Spring, MD) software. The following parameters were measured: (*1*) the number of glomerular nuclei and the total glomerular tuft cross-sectional area (gcsa) on H&E-stained slides (pilot study only), (*2*) the area of glomerular hematoxylin-positive nuclei and the total gcsa on H&E-stained slides, (*3*) the area of glomerular matrix and the total gcsa on silver methenamine–stained slides (pilot study only), and (*4*) the area of glomerular collagen IV matrix staining and the total gcsa. Results were expressed as the cell number per glomerular cross-section (gcs), the cell number per gcsa, the nuclear area per gcs, the percentage of nuclear area (area occupied by nuclei per gcsa), the area of collagen IV–positive matrix per gcs, and the percentage of collagen IV–positive matrix (area of collagen IV–positive matrix per gcsa).

The number of Mac-2–positive cells was counted in a minimum of 50 gcs. The expression of α-SMA was scored in a minimum of 50 gcs using a semiquantitative scale as described previously, with 0 = no staining, 1 = trace staining, 2 = <25% of the glomerular tuft positive, 3 = 25 to 75% of the glomerular tuft positive, and 4 = >75% of the tuft positive, and an overall average score was generated (26).

Electron Microscopy

Tissue fixed in half-strength Karnovsky's solution was processed, embedded, stained, and examined according to standard protocols as previously published (27, 28).

Mitogenic Assay

The mitogenic activity of purified PDGF-AA, -BB, -CC, and -DD was assessed by the ability to stimulate incorporation of [^{3}H]thymidine into normal human mesangial cells, as described previously (6). Cells were plated at a density of 2000 cells/well in 96-well culture plates and grown for approximately 72 h in DMEM containing 10% FCS. After incubation for 20 to 24 h in serum-free DMEM/Ham's F-12 medium containing insulin (5 μg/ml), transferrin (20 μg/ml), and selenium (16 pg/ml; ITS), medium was removed and test samples were added to the wells in triplicate. Test samples included 1 μg/ml, 100 ng/ml, 10 ng/ml, 1 ng/ml, 0.1 ng/ml, and 0.01 ng/ml of the following growth factors: PDGF-AA, PDGF-BB, PDGF-CC, and PDGF-DD, or appropriate buffer controls. For measurement of [^{3}H]thymidine incorporation, 20 μl of a 50-μCi/ml stock in DMEM was added directly to the cells, for a final activity of 1 μCi per well. After an additional 24-h incubation, mitogenic activity was assessed by measuring the uptake of [^{3}H]thymidine. Medium was removed, and cells were incubated with 0.1 ml of trypsin until cells detached. Cells were harvested onto 96-well filter plates using a sample harvester (FilterMate Harvester; Packard Instrument Co., Meriden, CT). The plates were then dried at 65°C for 15 min, sealed after adding 40 μl per well of scintillation fluid (Microscint O; Packard Instrument Co.), and counted on a microplate scintillation counter (Topcount; Packard Instrument Co.).

Statistical Analyses

Statistical analyses were performed using the SPSS program (Version 11.0 for Windows; SPSS, Inc., Chicago, IL). The means from the pilot study were compared using one-way ANOVA and Levene's test for homogeneity of variances. When variances were equal, the Tukey *post hoc* test was applied to determine significance. When variances were significantly different between the study groups, Tamhane *post hoc* test for significance was used. The small number of animals in each group of the time-course study ($n = 2$ or 4 at each time point) precluded statistical analysis of this portion of the overall set of studies. $P < 0.05$ was considered to be statistically significant. Graph error bars represent the SEM.

Results

Pilot Study

Mice overexpressing PDGF-D as a result of adenovirus-mediated gene transfer (Ad-D mice) developed a severe mesangial proliferative glomerulopathy characterized by a large increase in glomerular size and cellularity, as well as accumulation of extracellular matrix (Figure 1, D and H). The mice that received the Ad-PDGF-B construct (Ad-B mice) demonstrated a mild response, with slightly enlarged glomeruli and some accumulation of extracellular matrix (Figure 1, B and F). The mice that received the Ad-PDGF-C construct (Ad-C mice) and adenovirus-GFP construct (Ad control mice) showed no apparent pathology on histologic examination (Figure 1, A, C, E, and G).

Besides the kidney, other organs were affected by the circulating PDGF proteins. In mice that received the PDGF-B and PDGF-D adenoviruses, significant histopathologic changes were observed in the liver, bone, and lung. These included hepatic stellate cell proliferation and fibrosis in the liver, endosteal bone proliferation in long bones including the femur and humerus, and perivascular lymphoid cell infiltrates in the lung. The most severely affected organ in the mice that were exposed to the PDGF-C adenovirus was the liver, where hepatic stellate cell proliferation and fibrosis were observed. A detailed analysis of the morphologic alterations in liver will be presented in a separate article (in preparation).

Computer-aided morphometry was done to quantify changes within the kidney, including the average gcsa, average area of the glomerular tuft occupied by cell nuclei, the percentage of the glomerular tuft stained black with the silver methenamine stain, and the percentage of the glomerular tuft occupied by collagen IV–positive matrix in all study groups. The average gcsa in the Ad-D mice was 4632.5 (*versus* 2307.8 and 3578.5 μm^2 in untreated and adenovirus control animals, respectively; Table 2). The average number of cells per glomerular tuft was 108 in the Ad-D animals (*versus* 45 and 48 in the untreated and adenovirus control animals, respectively). As can be seen in Figure 1D, it is difficult to count the number of cells present in the glomeruli of the Ad-D mice because of the marked numerical increase and subsequent crowding of cells; as a consequence, the morphometry software used often counted groups of five to 10 nuclei as one cell because of their close proximity to one other. Generating accurate glomerular cell counts required a great deal of subjective manual manipulation within the software program to separate the clumps into single cells. To determine a more objective measure of glomerular cellularity, we repeated the morphometric measurements on all of the mice by measuring the total nuclear area (hematoxylin-positive area) per gcsa (Table 2). Comparison of the two measurements demonstrated a significant correlation between the cell number counted and the nuclear area measurement ($r^2 = 0.86$). Thus, we used this approach to quantify glomerular cellularity in the subsequent time-course study.

The average percentage of the glomerular tuft stained by silver methenamine in the pilot study Ad-D mice was 13.75% (*versus* 10.8 and 10.2% in the untreated and adenovirus control animals, respectively), and the percentage of the glomerular

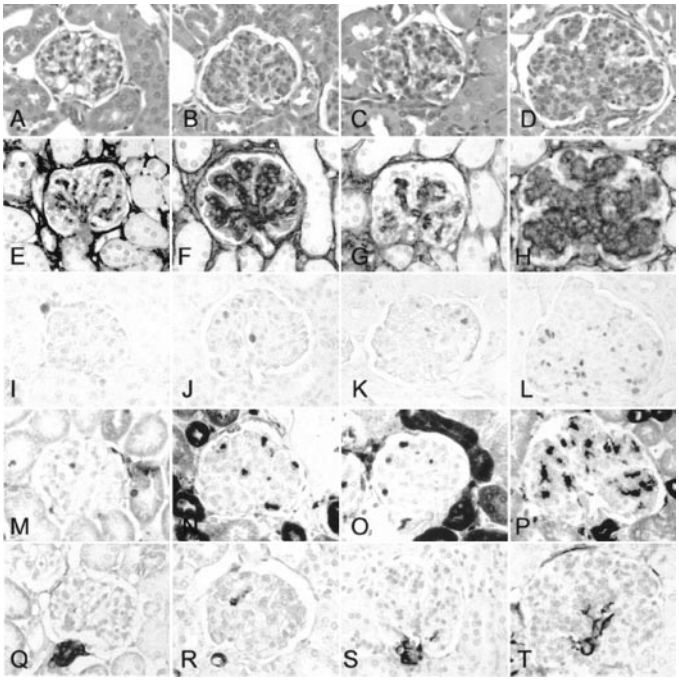

Figure 1. PDGF-B and PDGF-D cause mesangial proliferative glomerulopathy. Hematoxylin and eosin–stained glomeruli from representative mice (A through D), as well as representative glomeruli from tissue sections immunostained for collagen IV (E through H), Ki67 (I through L), Mac-2 (M through P), and α-smooth muscle actin (α-SMA; Q through T). (A, E, I, M, and Q) Glomeruli from an adenovirus alone control mouse shows normal histology with a well-defined mesangial stalk apparent in the collagen IV–immunostained section (B), few proliferating Ki-67–positive cells (I) or macrophages (M), and no glomerular actin expression (Q). (B, F, J, N, and R) Glomeruli from mice that received Ad-B have enlarged glomeruli and an increase in mesangial matrix, shown by the increase in dark staining material in the collagen IV–immunostained section (F). These mice also had an influx of glomerular macrophages (N) and an increase in α-SMA staining (R). (C, G, K, O, and S) Mice that received Ad-C seem essentially normal, with no increase in glomerular size or collagen IV accumulation. (D, H, L, P, and T) Mice that received Ad-D have extremely enlarged and hypercellular glomeruli (D) and have an accumulation of collagen IV matrix (H). The Ad-D mice also had significant increases in numbers of glomerular proliferating cells (L) and macrophages (P), as well as increased α-SMA expression (T). Magnification, $\times$400.

Table 2. Systemic levels of PDGF-B and PDGF-D result in enlarged, hypercellular glomeruli[a]

Pilot Study			
Group	Glomerular Cross-Sectional Area ($\mu m^2 \pm$ SEM)	Nuclear Area ($\mu m^2 \pm$ SEM)	Number of Cells Per Glomerular Cross-Section
Untreated	2821.1 ± 99.0	885.6 ± 30.6	45.3 ± 1.6
Adeno	3274.5 ± 125.9	1202.4 ± 77.6[d]	47.9 ± 2.4
Ad-B	4472.4 ± 206.5[b]	1706.9 ± 77.1[c]	77.9 ± 3.2[b]
Ad-C	3256.8 ± 129.4	1087.9 ± 46.8[d]	59.6 ± 2.4[c]
Ad-D	5765.5 ± 424.2[b]	2479.1 ± 156.9[c]	108.2 ± 8.5[b]

Time-Course Study-Mean Glomerular Cross-Sectional Area ($\mu m^2 \pm$ SEM)				
Group	2 Weeks	4 Weeks	6 Weeks	8 Weeks
Untreated	2633.7 ± 184.9	2610.5 ± 406.1	2990.2 ± 98.2	2831.7 ± 56.9
Adeno	2820.2 ± 178.6	2454.7 ± 113.3	3042.2 ± 123.2	2975.2 ± 59.3
Ad-B	3501.7 ± 161.7	3080.1 ± 137.9	3278.2 ± 178.6	3257.0 ± 278.0
Ad-C	3259.4 ± 289.8	3213.6 ± 144.0	2807.7 ± 207.1	3332.7 ± 253.5
Ad-D	5820.4 ± 139.9	4224.6 ± 283.8	3835.9 ± 166.0	4509.2 ± 228.2

Time-Course Study-Mean Glomerular Nuclear Area ($\mu m^2 \pm$ SEM)				
Group	2 Weeks	4 Weeks	6 Weeks	8 Weeks
Untreated	788.0 ± 128.7	784.7 ± 163.8	1032.0 ± 94.4	834.5 ± 13.3
Adeno	870.6 ± 87.8	686.0 ± 48.1	1033.4 ± 51.1	893.2 ± 11.0
Ad-B	1188.5 ± 126.4	1101.8 ± 114.3	1229.4 ± 103.6	1139.5 ± 89.2
Ad-C	1108.0 ± 230.6	858.9 ± 55.8	891.1 ± 75.2	983.7 ± 112.7
Ad-D	2350.5 ± 173.7	2283.7 ± 179.4	1752.9 ± 65.5	2012.9 ± 230.5

[a] Morphometry results of pilot and time-course study for glomerular area, glomerular nuclear area, and cells per glomerulus. [b]$P < 0.05$ *versus* untreated, adenovirus alone (Adeno), and Ad-C groups; [c]$P < 0.05$ *versus* all other groups; [d]$P < 0.05$ *versus* untreated.

tuft occupied by collagen IV–positive matrix was 33.52% (*versus* 20.2 and 17.3% in the untreated and adenovirus control animals, respectively; Figures 1H and 2B and not shown, Table 2). For technical reasons, either as a result of processing or the nature of the glomerular lesions, silver methenamine staining was inconsistent among the samples and did not adequately demonstrate the degree of matrix accumulation in the Ad-B and Ad-D animals, so we chose to use the production and accumulation of collagen IV within the mesangial matrix for morphometric measurements in the time-course study. For all of the histologic parameters measured (glomerular size, cellularity, and matrix accumulation), the mice that received the adenovirus PDGF-D construct were significantly different from all other groups except the PDGF-B mice ($P < 0.05$; Figure 2, A and B, Table 2).

The Ad-B mice in the pilot study had a mild increase in glomerular size (4343.5 μm^2), number of cells per glomerular tuft (78), and matrix accumulation (15.7% silver methenamine and 26.0% collagen IV; Figures 1, B and F, and 2, A and B, Table 2), and the increase in glomerular size and cellularity was statistically significant when compared with the mice that received the PDGF-C construct as well as the untreated and empty adenovirus controls ($P < 0.05$). The Ad-B mice had significant increases in mesangial collagen IV accumulation when compared with the adenovirus controls ($P < 0.05$; Figure 2B).

Mice that received the PDGF-C construct (Ad-C mice) had no significant increase in glomerular size, cell number, or matrix accumulation, but the glomerular cellularity (percentage of glomerular area occupied by nuclei) was increased when compared with the adenovirus control ($P < 0.05$; Figures 1, C and G, and 2, A and B, Table 2).

Control mice that received adenovirus alone (Ad mice) demonstrated no obvious histopathologic abnormalities, and although their glomeruli were slightly enlarged (3274.5 *versus* 2821.1 μm^2 in the untreated mice), the difference is not statistically significant, and there was no significant increase in glomerular cellularity or matrix accumulation when compared with the untreated mice (Figures 1, A and E, and 2, A and B, Table 2).

For better characterization of the identity of the cells present in the glomeruli of the Ad-D animals, tissue sections from all of the study animals were stained with cellular markers for macrophages (Mac-2), leukocytes (pan-leukocyte marker CD45), activated mesangial cells (α-SMA), and proliferating cells (Ki-67). In the Ad-D mice, there was a significant increase of both glomerular proliferating cells ($P < 0.05$ *versus* untreated, adenovirus alone and Ad-C; Figures 1L and 2C) and

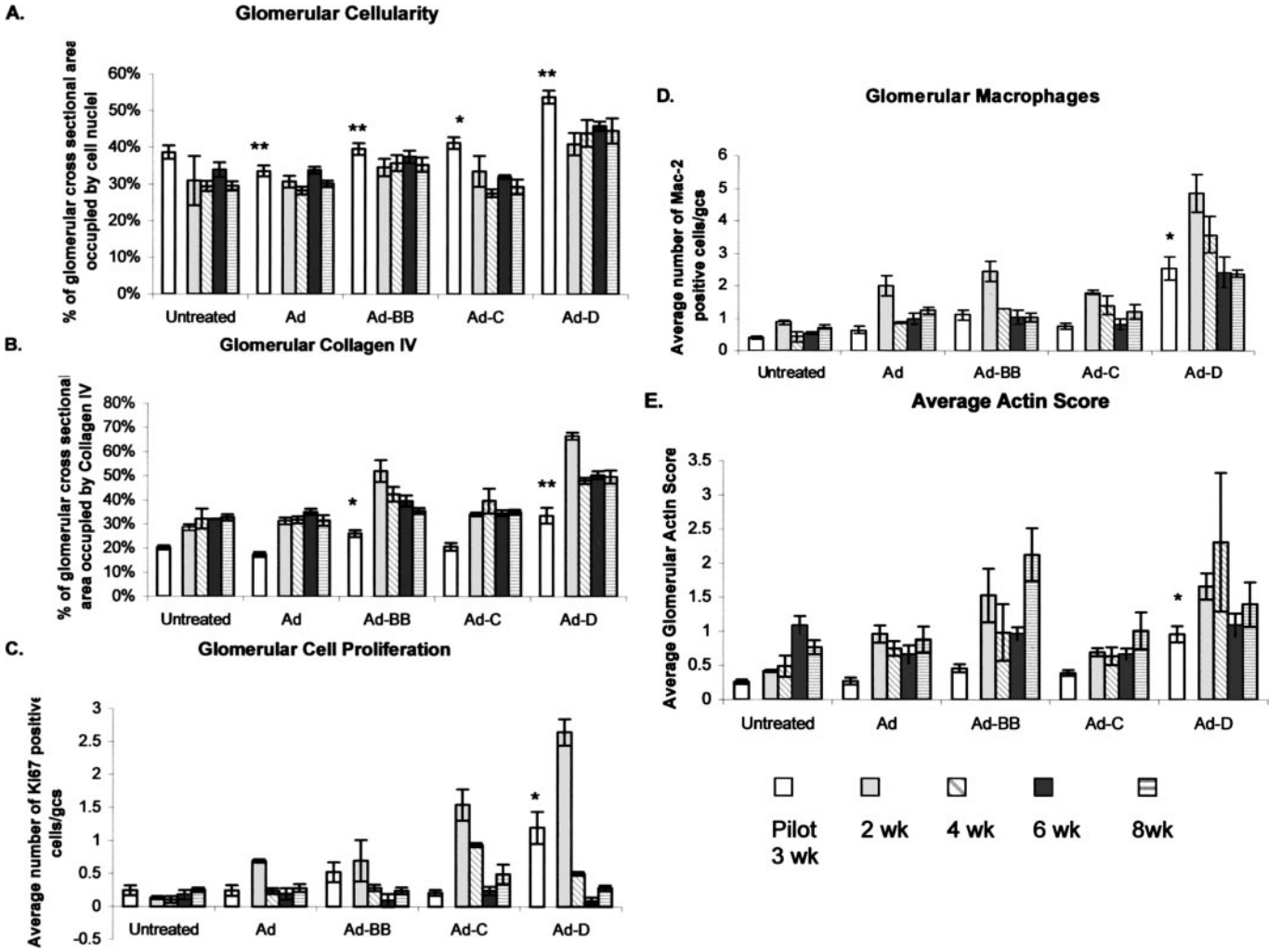

Figure 2. (A) Glomerular cellularity is increased in animals that received Ad-D. Morphometric analysis of glomerular cellularity (the percentage of the glomerular cross-sectional area [gcsa] occupied by hematoxylin-positive nuclei) demonstrates that the mice with high levels of circulating PDGF-D have an increase in overall glomerular cellularity. Shown are data from both the pilot study and the time-course study (*$P < 0.01$ *versus* adenovirus control [Ad]; **$P < 0.01$ *versus* Ad and Ad-D; #$P < 0.01$ *versus* all other groups; bars represent SEM). (B) Mice that received Ad-B and Ad-D have an increase in mesangial collagen IV–positive matrix. Morphometric analysis of the percentage of gcsa occupied by collagen IV. Data include the pilot study and the time-course study. The Ad-B and Ad-D mice have a significant increase in collagen IV matrix accumulation (*$P < 0.05$ *versus* Ad; **$P < 0.05$ *versus* all other groups; bars represent SEM). (C) Mice that received Ad-D have an increase in proliferating cells localized within glomeruli. Morphometric analysis of the average number of Ki-67–positive proliferating cells per glomerular cross-section (gcs). Data include the pilot study and the time-course study. The Ad-D mice have a significant increase in the number of proliferating cells per glomerulus, which decreases to normal levels over time in the 8-wk study (*$P < 0.05$ *versus* untreated, Ad, and Ad-C; bars represent SEM). (D) Mice that received Ad-B and Ad-D have an influx of glomerular macrophages. Morphometric analysis of the average number of Mac-2–positive macrophages per gcs. Data include the pilot study and the time-course study. The Ad-B and Ad-D mice have a large increase in glomerular macrophages, which decreases over time in the 8-wk study (*$P < 0.05$ *versus* all other groups; bars represent SEM). (E) Mice that received Ad-B and Ad-D have an increase in mesangial α-SMA expression. Analysis of the average glomerular actin score. Data include the pilot study and the time-course study. The Ad-B and Ad-D mice have a significant increase in α-SMA expression within glomeruli (*$P < 0.05$ *versus* all other groups; bars represent SEM).

glomerular macrophages ($P < 0.05$ *versus* all other groups; Figures 1P and 2D). These increases are not due simply to the increased glomerular size, as the numbers remain statistically significant when expressed as positive cells per average glomerular area (data not shown). There was not a substantial identifiable population of infiltrating leukocytes other than Mac-2–expressing monocyte/macrophages in the glomeruli of the Ad-D mice, as the immunostaining with the pan-leukocyte marker CD45 matched the pattern of Mac-2 staining (data not shown). The Ad-D mice also had significantly more α-SMA expressed in the glomerular tuft ($P < 0.05$ *versus* all other groups; Figures 1T and 2E). The Ad-B and Ad-C mice had slight increases in numbers of glomerular macrophages and proliferating cells, as well as glomerular actin expression, but these did not reach statistical significance (Figures 1, J, K, N, O, R, and S, and 2, C through E).

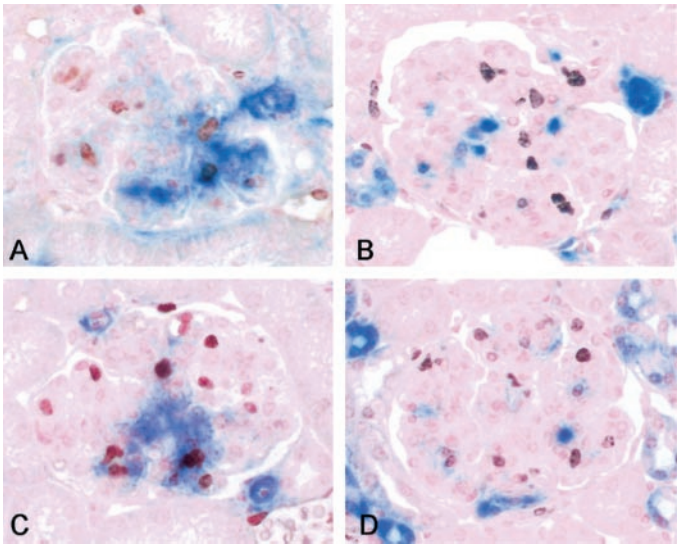

Figure 3. Double immunohistochemistry demonstrates proliferation by activated mesangial cells. (A and C) A mouse that received the Ad-D construct (2-wk time point) demonstrates association of Ki-67–positive proliferating cells (brown nuclei) with immunostaining for α-SMA (purple). (B and D) A sequential tissue section shows that proliferating cells (brown nuclei) are generally distinct from Mac-2–positive macrophages (purple). A and B and C and D represent two different Ad-D mice at 2-wk time point. Magnification, $\times$ 400.

The total amount of circulating PDGF varied widely depending on both the construct injected and the individual mouse (Table 3). The circulating levels of PDGF-BB achieved by the adenovirus gene transfer was at least 10-fold less than that obtained with the PDGF-C and PDGF-D constructs. Serum PDGF levels in the control mice were below the limits of detection. Despite the wide range of serum PDGF-D levels (range, 13.4 to 565.3 ng/ml), the pathology seen in the mice that received Ad-D construct was uniform, with no significant difference in glomerular size or cellularity between the mice with low (13.4 ng/ml) and high (565.4 ng/ml) serum levels of PDGF-D.

Table 3. Serum levels of PDGF-BB, PDGF-CC, and PDGF-DD are elevated in mice that received adenovirus constructs[a]

Ad-B Mice	BB ng/ml	SEM	Range
Ad-B Pilot	20.60	3.82	3.6–34.1
Ad-B 2 wk	8.05	4.80	0.4–22.1
Ad-B 4 wk	2.08	0.25	1.5–2.7
Ad-B 6 wk	1.98	0.17	1.6–2.3
Ad-B 8 wk	1.43	0.29	0.7–2.1
Ad-C Mice	**CC ng/ml**	**SEM**	**Range**
Ad-C Pilot	316.40	92.92	71–790
Ad-C 2 wk	122.90	33.50	80–200.1
Ad-C 4 wk	29.50	9.84	7.5–53.5
Ad-C 6 wk	5.95	2.56	1.9–13.4
Ad-C 8 wk	14.70	7.48	2.9–35.6
Ad-D Mice	**DD ng/ml**	**SEM**	**Range**
Ad-D Pilot	216.10	70.85	13.4–565.3
Ad-D 2 wk	1153.43	140.02	925.7–1554.9
Ad-D 4 wk	145.70	78.16	38–375
Ad-D 6 wk	23.75	3.03	17–31.4
Ad-D 8 wk	8.48	2.84	3.6–16.4

Ad Mice	BB ng/ml	CC ng/ml	DD ng/ml
Ad 2 wk	2.2	14	4
Ad 4 wk	3.2	0.0	1.6
Ad 6 wk	2.1	0.0	5.8
Ad 8 wk	2.5	1.5	2.8
Untreated Mice	**BB ng/ml**	**CC ng/ml**	**DD ng/ml**
Untreated 2 wk	nd	5.3	0.8
Untreated 4 wk	0.0	0.0	nd
Untreated 6 wk	nd	0.0	2.5
Untreated 8 wk	2.5	0.5	nd

[a] Serum levels of PDGF isoforms from mice in pilot study and time-course study as determined by ELISA assay.

Time-Course Study

The mice that received the Ad-D construct showed the same extreme glomerular proliferative response as was seen in the pilot study, with maximal pathology seen at the 2-wk time point. The Ad-B mice again demonstrated a mild response, with slightly enlarged glomeruli and some accumulation of extracellular matrix. The Ad-C and adenovirus control mice showed no apparent pathology on histologic examination.

Computer-aided morphometry was done to quantify the average gcsa, average area of the glomerular tuft occupied by cell nuclei, and the percentage of the glomerular tuft occupied by collagen IV–positive matrix in all study groups. Glomeruli in the 2-wk Ad-D group were enlarged (average, 5820 *versus* 2634 μm^2 in untreated control mice) and so hypercellular that virtually no patent capillary loops could be seen. Immunostaining of collagen IV demonstrated a marked accumulation of extracellular matrix in the Ad-B and Ad-D mice (Figure 2B). In the Ad-D mice, glomerular size, glomerular nuclear area, and matrix accumulation were maximal at 2 wk after injection and then decreased somewhat during the subsequent 6-wk time course (Figure 2, A and B, Table 2). As in the pilot study, the Ad-B mice had a milder response, with a slight to moderate increase in glomerular size, glomerular cellularity, and collagen IV accumulation (Figure 2, A and B, Table 2). The Ad-C mice also had a slight increase in glomerular size and cellularity at the 2-wk time point compared with untreated controls; however, these parameters returned to normal at the subsequent time points (Figure 2A, Table 2). Mice that received

adenovirus alone showed no significant increase in glomerular size, cellularity, or collagen IV accumulation when compared with the untreated controls (Figure 2, A and B, Table 2).

Immunohistochemistry revealed that the Ad-D mice had a large glomerular macrophage influx at the 2-wk time point with an average of 4.85 ± 1.18 macrophages per glomerulus (Figure 2D). The number of macrophages per glomerulus decreased during the subsequent time course of the study but remained elevated at 8 wk (2.4 ± 0.25) when compared with the adenovirus (1.2 ± 0.2) or untreated (0.7 ± 0.08) control mice at 8 wk. The Ad-B mice, Ad-C mice, and Ad control mice also had a mild glomerular macrophage influx at the 2-wk time point (2.4 ± 0.6, 1.8 ± 0.1, and 2.0 ± 0.3 macrophages per glomerulus, respectively), and by the end of the study period, both of these groups had macrophage numbers similar to those of the untreated control mice. As in the pilot study, CD45 immunostaining revealed that macrophages constituted the vast majority of the infiltrating leukocytes, as the number of CD45-positive cells was essentially equivalent to the number of Mac-2–positive cells within the glomeruli of all mice (data not shown). There was no significant influx of neutrophils or T cells into the kidneys of any of the groups (data not shown).

Similar to the pilot study, the Ad-D mice had an increase in the number of proliferating (Ki-67 positive) cells localized within the glomerulus at the 2-wk time point when compared with all other groups. (Figure 2C). The number of glomerular proliferating cells decreased rapidly and were at control levels at 4, 6, and 8 wk. The Ad-B, Ad-C, and adenovirus control mice also had increased numbers of proliferating cells at the 2-wk time point, but the numbers also decreased to control levels during the subsequent time course.

Expression of α-SMA is generally acknowledged to be a marker of mesangial cell activation. In the time-course study, both the Ad-D and -BB mice showed increases in mesangial SMA staining, whereas the Ad-C, Ad, and control mice all had minimal glomerular actin expression (Figure 2E). Although the expression of α-SMA remained elevated in the Ad-B and -D mice during the 8-wk time course, there were large variances within these groups.

There was no difference in the expression patterns of WT-1, a marker of visceral epithelial cells, and CD31, a marker of endothelial cells, among the various groups (data not shown), demonstrating that these cell types were not contributing to the hypercellularity seen in the Ad-D mice.

Double immunohistochemistry was done to identify the proliferating cells within the glomeruli of the Ad-D mice. The proliferating, Ki-67–positive nuclei often co-localized with α-SMA and were mostly distinct from the Mac-2–positive macrophages within glomeruli (Figure 3), indicating that the majority of the identifiable proliferating cells within the glomerular tuft were mesangial cells and not circulating monocyte/macrophages. There were also a number of Ki-67–positive cells that did not co-localize with either α-SMA or Mac-2, and thus their identity remains unknown.

Immunohistochemistry was performed with antibodies directed against PDGF-B, PDGF-D, and PDGFR-β. PDGF-D was expressed constitutively by mesangial cells and vascular smooth muscle cells in all mice (Figure 4, A and E, and data not shown). The expression or accumulation of PDGF-D was increased in glomeruli of both the Ad-B and -D mice, consistent with a mesangial pattern, although we cannot be certain that all of the staining was within the mesangium (Figure 4A). PDGF-B and PDGFR-β were also localized in a mesangial pattern in all of the mice and seemed to be increased in both the Ad-B and Ad-D mice (Figure 4, B and C). The glomerular expression pattern of PDGF-D matched the expression pattern of PDGF-B, PDGFR-β, and collagen IV (Figure 4, A through D).

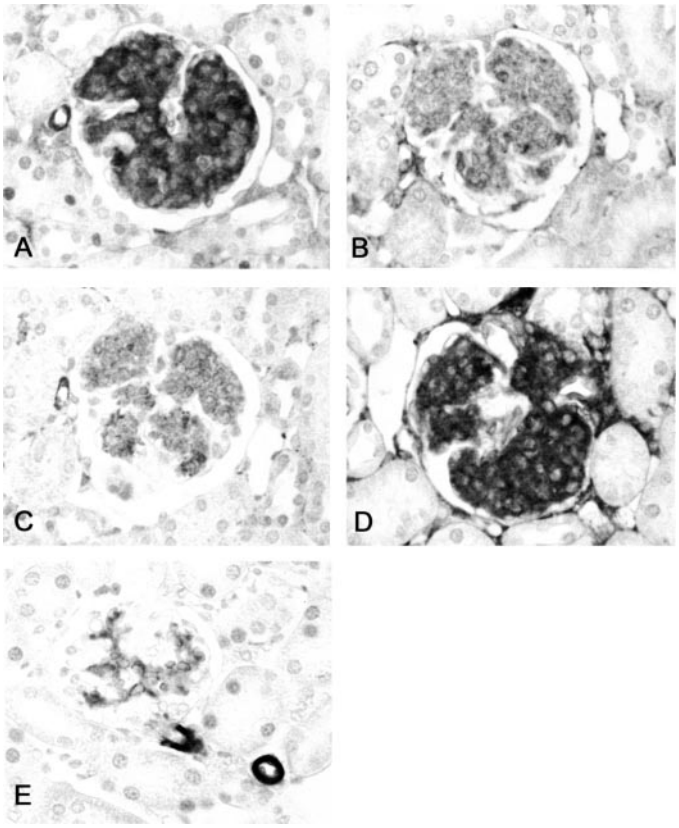

Figure 4. PDGF-D protein localizes in a predominantly mesangial pattern and co-localizes with PDGF-B and PDGFR-β. (A) Immunolocalization of PDGF-D in a mouse that received the Ad-D construct demonstrates increased glomerular expression of PDGF-D (compare with E). (B) PDGFR-β co-localizes with PDGF-D in a sequential tissue section. (C) PDGF-B is also localized in a similar pattern in a sequential section. (D) Collagen IV immunostaining in subsequent tissue section shows localization of mesangial matrix in a pattern identical to those of PDGF-D, PDGF-B, and PDGFR-β. (E) Immunolocalization of PDGF-D in an adenovirus-only control mouse shows PDGF-D expression in the mesangial stalk and vascular smooth muscle cells. Magnification, ×400.

TUNEL staining was performed on tissue sections from the Ad-D mice, as well as from the Ad and untreated control mice. The Ad-D and control mice had a similar number of TUNEL-positive cells within the glomerular tuft at the 2-wk time point (average, 0.025 ± 0.013 *versus* 0.028 ± 0.02 and 0.0 in the adenovirus and untreated control mice). At the 4-wk time

point, the Ad-D mice had an average of 0.06 ± 0.015 TUNEL-positive cells per glomerulus (*versus* 0.01 in both adenovirus and untreated control mice). At 6 wk, the Ad-D mice had 0.022 ± 0.017 TUNEL-positive cells per glomerulus (*versus* 0.028 ± 0.022 and 0.012 ± 0.010 in the adenovirus and untreated control mice, respectively). At the 8-wk time point, the Ad-D mice had 0.047 ± 0.022 TUNEL-positive cells per glomerulus (*versus* 0.041 ± 0.023 and 0.025 ± 0.013 in the adenovirus and untreated control mice, respectively). When all of the data from all four time points are averaged, the Ad-D mice had 0.04 ± 0.022 TUNEL-positive cells per glomerulus, whereas the Ad control mice had 0.027 ± 0.022 and the untreated control mice had 0.01 ± 0.012 TUNEL-positive cells per glomerulus. When adjusted for differences in glomerular size, there was no significant difference between the groups (data not shown).

Electron microscopy was performed on two of the Ad-D mice (2-wk and 8-wk time points) and one Ad control mouse (2-wk time point). At the 2-wk time point, the glomeruli of the PDGF-D mice had a greatly expanded mesangium, with accumulation of both mesangial cells and matrix (Figure 5A), with encroachment of the expanded mesangium into adjacent capillary loops. There was little evidence of immune complex deposition in either the mesangium or the capillary basement membranes (Figure 5B), although rare, small, ill-defined electron densities in mesangial regions were identified. There was also focal effacement of visceral epithelial cell foot processes (Figure 5B, inset). At 8 wk, the Ad-D mice (Figure 5C) still had an expanded mesangium when compared with the adenovirus control (Figure 5D) and reduction of the extent of mesangial expansion compared with animals from the 2-wk time point, in concordance with the histologic findings.

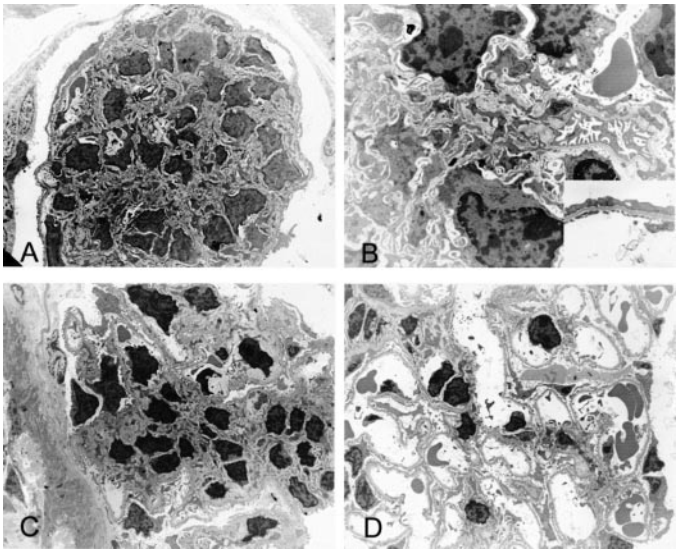

Figure 5. Electron microscopy demonstrates mesangial proliferation in mice that received PDGF-D adenovirus construct. (A) Low-power view of a glomerulus from a PDGF-D mouse at the 2-wk time point shows accumulation of mesangial cells and matrix. (B) Higher-power view of A. Inset shows effacement of visceral epithelial cells. (C) A PDGF-D mouse at 8 wk shows a reduction in the mesangial expansion compared with the 2-wk time point. (D) Low-power view of a mouse that received adenovirus alone at 2 wk after injection shows normal glomerular histology. Magnifications: ×1600 in A, C, and D; ×3000 in B; ×10,400 in inset.

As in the pilot study, the circulating serum levels of PDGF varied widely among the various isoforms and also from animal to animal (Table 3). The serum levels of PDGF-BB were relatively low at 2 wk in the Ad-B mice (average, 8.05 ng/ml; range, 0.4 to 22.1 ng/ml) and dropped off to levels equivalent to the untreated mice by the end of the study (average, 1.4 ng/ml; range, 0.7 to 2.1 ng/ml). The Ad-C mice had circulating PDGF-C levels averaging 123 ng/ml at 2 wk (range, 80 to 200.1 ng/ml), which dropped to an average of 14.7 ng/ml at 8 wk (range, 2.9 to 35.6 ng/ml). At 2 wk, the Ad-D mice had very high levels of serum PDGF-D (average, 1153.4 ng/ml; range, 925.7 to 1554.9 ng/ml), dropping to an average of 8.5 ng/ml by 8 wk (range, 3.6 to 16.4 ng/ml). The average serum levels of PDGF-B, -C, and -D in the adenovirus and untreated control mice are shown in Table 3, with serum levels of all PDGF isoforms generally <5 ng/ml in the control mice.

Blood chemistry was analyzed at the time that the mice were killed, and serum creatinine, blood urea nitrogen, albumin, and globulin levels demonstrated that despite the histopathology observed in the Ad-B and Ad-D mice, there was no significant decrease in renal function in any of the study groups (Table 4 and data not shown).

In Vitro Studies

The mitogenic activity of purified PDGF-AA, -BB, -CC, and -DD was assessed by their ability to stimulate incorporation of [^{3}H]thymidine into growth-arrested human mesangial cells. As shown in Figure 6, PDGF-BB, -CC, and -DD all led to significant induction of mesangial cell proliferation at 0.01 ng/ml that resulted in an approximate twofold increase of tritiated thymidine incorporation *versus* media alone. All three growth factor isoforms demonstrated very similar dose-dependent effects, which plateaued at 10 to 100 ng/ml, with an increased tritium incorporation of sevenfold (PDGF-BB and -DD) to 10-fold (PDGF-CC) at these higher concentrations. In this experiment, PDGF-AA resulted in a weak mitogenic response in the mesangial cells at all of the concentrations tested (0.01 to 1 μg/ml) and was statistically significant at 1 and 10 ng/ml ($P < 0.05$ *versus* media alone).

Discussion

The recent discovery of two new members of the PDGF family, PDGF-C and -D, has provided us the opportunity to explore the role of these growth factors in renal disease. There is some evidence that PDGF-C expression is upregulated in both rodent models of injury and in human disease and hence may play a role in mesangial injury and repair (19, 20), but to date, nothing is known about a potential role for PDGF-D. In this study, adenovirus constructs were used to introduce the coding regions of PDGF-BB, -C, and -D into mice, which resulted in an increase in circulating serum levels of each of these growth factors, providing a means to determine the renal response to exogenous PDGF.

The major finding of this study is that all of the mice that

Table 4. Serum creatinine and BUN values, time-course study[a]

	2 Weeks	4 Weeks	6 Weeks	8 Weeks
Serum creatinine ± SEM				
untreated	0.250 ± 0.050	0.450 ± 0.050	0.200 ± 0.000	0.300 ± 0.100
Adeno	0.375 ± 0.025	0.250 ± 0.050	0.200 ± 0.000	0.200 ± 0.000
Ad-B	0.375 ± 0.025	0.350 ± 0.050	0.150 ± 0.050	0.200 ± 0.000
Ad-C	0.400 ± 0.000	0.375 ± 0.025	0.350 ± 0.095	0.200 ± 0.000
Ad-D	0.350 ± 0.050	0.375 ± 0.050	0.200 ± 0.000	0.250 ± 0.050
Serum BUN ± SEM				
untreated	22.00 ± 2.00	28.00 ± 4.00	26.00 ± 4.00	31.00 ± 1.00
Adeno	25.75 ± 0.85	31.00 ± 1.73	25.50 ± 1.70	30.00 ± 1.83
Ad-B	31.25 ± 1.11	24.50 ± 2.06	24.50 ± 0.50	26.00 ± 2.58
Ad-C	24.25 ± 2.39	30.50 ± 2.06	31.00 ± 6.56	35.00 ± 2.89
Ad-D	32.00 ± 4.38	41.75 ± 2.17	27.50 ± 1.26	34.00 ± 3.56

BUN, blood urea nitrogen.

[a] Statistical analysis of each treatment group across the four time points showed no difference across the time course of the study for either parameter. The data for all time points were combined for each treatment group and analyzed by one-way ANOVA, revealing no statistically significant differences between the groups.

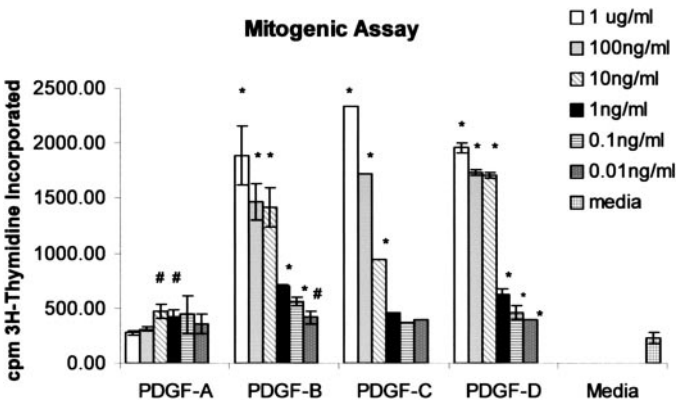

Figure 6. PDGF-BB, -CC, and -DD are mitogenic for mesangial cells *in vitro*. [^{3}H]thymidine incorporation into growth-arrested human mesangial cells that were stimulated with 0.01 to 1 mg/ml PDGF-AA, -BB, -CC, or -DD or with control media. Data are mean ± SEM of triplicate experiments, except for PDGF-CC, which was a single experiment. *$P < 0.01$ *versus* media control; #$P < 0.05$ *versus* media control.

were exposed to exogenous PDGF-D, regardless of the serum level of PDGF-D, developed an extreme mesangial proliferative glomerulopathy, with enlarged and hypercellular glomeruli. As shown by immunohistochemistry, the glomeruli of these mice had a macrophage influx, accumulation of extracellular matrix, and an increase in proliferating cells. The Ad-D mice had increased glomerular expression of α-SMA, a phenotypic marker of mesangial cell activation (23, 29, 30). Electron microscopy demonstrated that the majority of cells present within these extremely hypercellular glomeruli were in fact mesangial cells, and double immunohistochemistry showed that many of the Ki-67–positive proliferating cells within the glomeruli were α-actin–expressing mesangial cells and not monocyte/macrophages. Because there was no apparent increase in other leukocytes or in intrinsic renal cells (endothelial cells or visceral epithelial cells) as shown by further immunohistochemistry for these cell types, it seems to us likely that the remaining population of Ki-67–positive, actin-negative cells were also mesangial cells that did not express α-SMA. As the serum levels of PDGF-D declined during the time course of the study, there was some resolution of the glomerular damage. The glomeruli were smaller, were less hypercellular, and had more patent capillary loops at 8 wk after Ad-D injection when compared with 2 wk after injection. This suggests that without continuous stimulation by PDGF-D, the glomerulus is able to undergo a repair process that at least partially ameliorates the mesangial proliferative pathology seen in these animals. TUNEL staining demonstrated a slight increase in apoptotic cells within the glomeruli of the Ad-D mice when compared with the adenovirus and untreated control mice, indicating a possible mechanism by which affected glomeruli returned to normocellularity. Because of the temporal limits of the study, it is unknown whether the glomeruli of these mice would return to complete normality or interstitial fibrosis would develop over a longer period of time. There was an increase in tubular epithelial cell proliferation (Ki-67 staining) in these mice but no other features of a specific tubulointerstitial injury. Finally, the discordance between the remarkable histopathologic changes and the unaltered measures of renal function observed in this portion of the study demonstrate the ability of the kidney to functionally tolerate an acute, severe mesangial proliferative glomerulopathy and underscores the limited sensitivity of some measures of renal function, such as serum creatinine, to detect significant glomerular injury.

Despite relatively high levels of serum PDGF-CC, the mice that were administered the PDGF-CC adenoviral construct showed no evidence of renal pathology. It was demonstrated recently that PDGF-C is constitutively expressed in vascular smooth muscle cells and collecting duct epithelium in rat kidney and that its expression is upregulated in the mesangial

cells of rats in the Thy1.1 model of mesangioproliferative glomerulonephritis (19). In concordance with results reported in that study, we demonstrate that PDGF-C is a potent mesangial cell mitogen *in vitro*. It is therefore puzzling (but unexplained) that the Ad-C mice in this study lacked any significant renal pathology.

The mice that received the PDGF-BB adenovirus vector did not attain the high circulating serum levels seen in the Ad-C and Ad-D mice. Despite lower levels of serum PDGF-B, the glomeruli of these mice demonstrated a mesangial proliferative response, with a significant increase in glomerular size and matrix accumulation as well as increased numbers of glomerular proliferating cells, macrophage influx, and increased mesangial actin expression. These observations are consistent with other studies that demonstrated mesangial cell proliferation and matrix accumulation in rats that were infused with PDGF-BB (15) or rats that overexpressed PDGF-BB in their kidney after *in vivo* transfection (31). We recognize that observed differences in renal pathology between Ad-D and Ad-B mice may indicate a true biologic difference but also may be attributable to differences in the systemic levels of overexpressed peptides that were achieved and perhaps to differences in bioavailability as a result of binding to other circulating plasma proteins. Hence, differences in the apparent efficacy of PDGF-BB and -DD in mediating mesangial proliferation *in vivo* in this study need to be interpreted with caution, especially given the similarity of mesangial proliferative responses to these two isoforms *in vitro*.

A potential cause of the differences seen in systemic levels of the various PDGF isoforms may be a consequence of the adenovirus delivery system that was used. Adenoviruses are one of several viruses that have been used as gene delivery vectors in experimental and clinical gene therapy (32) and as one of the few strategies available for specifically targeting the kidney (33, 34). As seen in the present study, the time period of expression of the transfected gene is generally limited to weeks or months, as the adenovirus does not integrate into the host genome. The adenovirus vectors used in this study were not specifically targeted to the kidney but were introduced intravenously, and the majority of gene expression was seen in the liver. The renal effects thus were due primarily to circulating PDGF and not to direct expression of PDGF-B, -C, or -D by intrinsic renal cells. It is not clear why there was such a wide variation in the serum levels achieved with the different vectors and even among different mice that received the same vector. One of the intrinsic problems with using adenovirus vectors is their ability to elicit an immune response in the host animal. It is possible that local immune/inflammatory responses at the site of vector localization and gene expression may be the cause of diminished or extinguished gene activity. Thus, the variations in serum level seen among animals that received the same vector may reflect differences in specific and humoral immune responses that mediate clearance of adenovirus-infected cells. Another possibility is variation in binding to circulating plasma proteins such as albumin.

An important finding of this study was a discrepancy between sites of renal expression of PDGF-D in humans *versus* mice. In the human kidney, PDGF-D is expressed constitutively by visceral epithelial cells and vascular smooth muscle cells but not in mesangial cells (21). In contrast, immunostaining of mouse kidney performed with the same antibody used in the human studies demonstrated constitutive expression of PDGF-D by mesangial cells and not glomerular epithelial cells. Constitutive expression of PDGF-D by vascular smooth muscle cells was similar to that seen in humans. We previously identified molecules with constitutive expression in the glomerulus in which the principal cell type expressing the molecule alternated between mesangial cells in rodent species and visceral epithelial cells in humans, and *vice versa* (*e.g.*, p75 nerve growth factor receptor (35) [unpublished results in rodents] and PTPRQ, a newly discovered phosphatase (36)). In the proliferative lesions of the Ad-B and Ad-D mice, immunolocalization of PDGF-D was increased in the mesangium in concert with an increase in PDGF-B and PDGFR-β expression. Thus, in the mouse, PDGF-D may act in concert with or compete with PDGF-B in autocrine signaling within the mesangium.

In conclusion, the principal findings of this study are *in vivo* and *in vitro* evidence that PDGF-D alone is a potent mitogen for mesangial cells but not other cell types in the kidney and that PDGF-D can initiate events that lead to a mesangial proliferative glomerulonephritis, including influx of monocyte/macrophages and production of extracellular matrix. The predictable and florid features of the induced glomerulonephritis and relatively short interval between introduction of the adenoviral construct and development of morphologic disease make this a particularly attractive model for studies of mesangial proliferative injury and its repair. Comparative studies yielded the somewhat surprising finding that overexpression of PDGF-C did not result in any significant injury, despite its ability to cause mesangial cell proliferation *in vitro*. In conjunction with the finding that overexpression of PDGF-B also is sufficient to produce a mesangioproliferative injury, our study emphasizes a key role for PDGFR-β, through which both PDGF-B and -D signal, in mediating mesangial proliferative diseases.

Acknowledgments

Support for this study was provided by a National Institutes of Health–funded O'Brien Kidney Center of Research Excellence grant (DK 47659) and by a grant from ZymoGenetics, Inc. A portion of this work was presented as an abstract at the meeting of the American Society of Nephrology, Philadelphia, 2002.

We thank Barbara Gutierrez and Heather Day for the adenovirus constructs.

References

1. Johnson R, Iida H, Yoshimura A, Floege J, Bowen-Pope DF: Platelet-derived growth factor: A potentially important cytokine in glomerular disease. *Kidney Int* 41: 590–594, 1992
2. Johnson RJ, Floege J, Couser WG, Alpers CE: Role of platelet-derived growth factor in glomerular disease. *J Am Soc Nephrol* 4: 119–128, 1993

3. Alpers CE, Johnson RJ: Growth factors and the glomerulus: Relationships between development and injury. *Adv Nephrol Necker Hosp* 24: 33–52, 1995
4. Floege J, Topley N, Resch K: Regulation of mesangial cell proliferation. *Am J Kidney Dis* 17: 673–676, 1991
5. Floege J, Topley N, Hoppe J, Barrett TB, Resch K: Mitogenic effect of platelet-derived growth factor in human glomerular mesangial cells: Modulation and/or suppression by inflammatory cytokines. *Clin Exp Immunol* 86: 334–341, 1991
6. Gilbertson DG, Duff ME, West JW, Kelly JD, Sheppard PO, Hofstrand PD, Gao Z, Shoemaker K, Bukowski TR, Moore M, Feldhaus AL, Humes JM, Palmer TE, Hart CE: Platelet-derived growth factor C (PDGF-C), a novel growth factor that binds to PDGF alpha and beta receptor. *J Biol Chem* 276: 27406–27414, 2001
7. LaRochelle WJ, Jeffers M, McDonald WF, Chillakuru RA, Giese NA, Lokker NA, Sullivan C, Boldog FL, Yang M, Vernet C, Burgess CE, Fernandes E, Deegler LL, Rittman B, Shimkets J, Shimkets RA, Rothberg JM, Lichenstein HS: PDGF-D, a new protease-activated growth factor. *Nat Cell Biol* 3: 517–521, 2001
8. Li X, Ponten A, Aase K, Karlsson L, Abramsson A, Uutela M, Backstrom G, Hellstrom M, Bostrom H, Li H, Soriano P, Betsholtz C, Heldin CH, Alitalo K, Ostman A, Eriksson U: PDGF-C is a new protease-activated ligand for the PDGF alpha-receptor. *Nat Cell Biol* 2: 302–309, 2000
9. Heldin CH, Westermark B: Mechanism of action and in vivo role of platelet-derived growth factor. *Physiol Rev* 79: 1283–1316, 1999
10. Hart CE, Forstrom JW, Kelly JD, Seifert RA, Smith RA, Ross R, Murray MJ, Bowen-Pope DF: Two classes of PDGF receptor recognize different isoforms of PDGF. *Science* 240: 1529–1531, 1988
11. Seifert RA, Hart CE, Phillips PE, Forstrom JW, Ross R, Murray MJ, Bowen-Pope DF: Two different subunits associate to create isoform-specific platelet-derived growth factor receptors. *J Biol Chem* 264: 8771–8778, 1989
12. Claesson-Welsh L, Eriksson A, Moren A, Severinsson L, Ek B, Ostman A, Betsholtz C, Heldin CH: cDNA cloning and expression of a human platelet-derived growth factor (PDGF) receptor specific for B-chain-containing PDGF molecules. *Mol Cell Biol* 8: 3476–3486, 1988
13. Floege J, Ostendorf T, Wolf G: Growth factors and cytokines. In: *Immunologic Renal Diseases*, edited by Neilson EG, Couser WG, 2nd Ed., Baltimore, Lippincott Williams & Wilkins, 2001
14. Johnson RJ, Floege J, Couser WG, Alpers CE: Role of platelet-derived growth factor in glomerular disease [Editorial]. *J Am Soc Nephrol* 4: 119–128, 1993 [published erratum appears in *J Am Soc Nephrol* 4: 1237, 1993]
15. Floege J, Eng E, Young BA, Alpers CE, Barrett TB, Bowen-Pope DF, Johnson RJ: Infusion of platelet-derived growth factor or basic fibroblast growth factor induces selective glomerular mesangial cell proliferation and matrix accumulation in rats. *J Clin Invest* 92: 2952–2962, 1993
16. Floege J, Ostendorf T, Janssen U, Burg M, Radeke HH, Vargeese C, Gill SC, Green LS, Janjic N: Novel approach to specific growth factor inhibition in vivo: Antagonism of platelet-derived growth factor in glomerulonephritis by aptamers. *Am J Pathol* 154: 169–179, 1999
17. Iida H, Seifert R, Alpers CE, Gronwald RG, Phillips PE, Pritzl P, Gordon K, Gown AM, Ross R, Bowen-Pope DF, *et al.*: Platelet-derived growth factor (PDGF) and PDGF receptor are induced in mesangial proliferative nephritis in the rat. *Proc Natl Acad Sci U S A* 88: 6560–6564, 1991
18. Ostendorf T, Kunter U, Grone HJ, Bahlmann F, Kawachi H, Shimizu F, Koch KM, Janjic N, Floege J: Specific antagonism of PDGF prevents renal scarring in experimental glomerulonephritis. *J Am Soc Nephrol* 12: 909–918, 2001
19. Eitner F, Ostendorf T, Van Roeyen C, Kitahara M, Li X, Aase K, Grone HJ, Eriksson U, Floege J: Expression of a novel PDGF isoform, PDGF-C, in normal and diseased rat kidney. *J Am Soc Nephrol* 13: 910–917, 2002
20. Eitner F, Ostendorf T, Kretzler M, Cohen CD, Eriksson U, Grone HJ, Floege J: PDGF-C Expression in the developing and normal adult human kidney and in glomerular diseases. *J Am Soc Nephrol* 14: 1145–1153, 2003
21. Changsirikulchai S, Hudkins KL, Goodpaster TA, Volpone J, Topouzis S, Gilbertson DG, Alpers CE: Platelet-derived growth factor-D expression in developing and mature human kidneys. *Kidney Int* 62: 2043–2054, 2002
22. Hudkins KL, Giachelli CM, Cui Y, Couser WG, Johnson RJ, Alpers CE: Osteopontin expression in fetal and mature human kidney. *J Am Soc Nephrol* 10: 444–457, 1999
23. Alpers CE, Hudkins KL, Gown AM, Johnson RJ: Enhanced expression of "muscle-specific" actin in glomerulonephritis. *Kidney Int* 41: 1134–1142, 1992
24. Alpers CE, Seifert RA, Hudkins KL, Johnson RJ, Bowen-Pope DF: Developmental patterns of PDGF B-chain, PDGF-receptor, and alpha-actin expression in human glomerulogenesis. *Kidney Int* 42: 390–399, 1992
25. Segerer S, Eitner F, Cui Y, Hudkins KL, Alpers CE: Cellular injury associated with renal thrombotic microangiopathy in human immunodeficiency virus-infected macaques. *J Am Soc Nephrol* 13: 370–378, 2002
26. Taneda S, Pippin JW, Sage EH, Hudkins KL, Takeuchi Y, Couser WG, Alpers CE: Amelioration of diabetic nephropathy in SPARC-null mice. *J Am Soc Nephrol* 14: 968–980, 2003
27. Alpers CE, Hudkins KL, Pritzl P, Johnson RJ: Mechanisms of clearance of immune complexes from peritubular capillaries in the rat. *Am J Pathol* 139: 855–867, 1991
28. Eitner F, Cui Y, Hudkins KL, Schmidt A, Birkebak T, Agy MB, Hu SL, Morton WR, Anderson DM, Alpers CE: Thrombotic microangiopathy in the HIV-2-infected macaque. *Am J Pathol* 155: 649–661, 1999
29. Johnson RJ, Floege J, Yoshimura A, Iida H, Couser WG, Alpers CE: The activated mesangial cell: a glomerular "myofibroblast"? *J Am Soc Nephrol* 2[Suppl]: S190–S197, 1992
30. Johnson RJ, Iida H, Alpers CE, Majesky MW, Schwartz SM, Pritzi P, Gordon K, Gown AM: Expression of smooth muscle cell phenotype by rat mesangial cells in immune complex nephritis. Alpha-smooth muscle actin is a marker of mesangial cell proliferation. *J Clin Invest* 87: 847–858, 1991
31. Isaka Y, Fujiwara Y, Ueda N, Kaneda Y, Kamada T, Imai E: Glomerulosclerosis induced by in vivo transfection of transforming growth factor-beta or platelet-derived growth factor gene into the rat kidney. *J Clin Invest* 92: 2597–2601, 1993
32. Lotze MT, Kost TA: Viruses as gene delivery vectors: Application to gene function, target validation, and assay development. *Cancer Gene Ther* 9: 692–699, 2002
33. McDonald GA: Targeted adenoviral gene transfer to the kidney. *Kidney Int Suppl* 61[Suppl 1]: 42–46, 2002

34. Imai E: Gene therapy approach in renal disease in the 21st century. *Nephrol Dial Transplant* 16[Suppl 5]: 26–34, 2001
35. Seifert RA, Coats SA, Oganesian A, Wright MB, Dishmon M, Booth CJ, Johnson RJ, Alpers CE, Bowen-Pope DF: PTPRQ is a novel phosphatidylinositol phosphatase that can be expressed as a cytoplasmic protein or as a subcellularly localized receptor-like protein. *Exp Cell Res* 287: 374–386, 2003
36. Rosenberg I, Cherayil BJ, Isselbacher KJ, Pillai S: Mac-2-binding glycoproteins. Putative ligands for a cytosolic beta-galactoside lectin. *J Biol Chem* 266: 18731–18736, 1991
37. Segerer S, Hudkins KL, Taneda S, Wen M, Cui Y, Segerer M, Farr AG, Alpers CE: Oral interferon-alpha treatment of mice with cryoglobulinemic glomerulonephritis. *Am J Kidney Dis* 39: 876–888, 2002
38. Taneda S, Segerer S, Hudkins KL, Cui Y, Wen M, Segerer M, Wener MH, Khairallah CG, Farr AG, Alpers CE: Cryoglobulinemic glomerulonephritis in thymic stromal lymphopoietin transgenic mice. *Am J Pathol* 159: 2355–2369, 2001
39. Vanzulli S, Gazzaniga S, Braidot MF, Vecchi A, Mantovani A, Wainstok de Calmanovici R: Detection of endothelial cells by MEC 13.3 monoclonal antibody in mice mammary tumors. *Biocell* 21: 39–46, 1997
40. Vecchi A, Garlanda C, Lampugnani MG, Resnati M, Matteucci C, Stoppacciaro A, Schnurch H, Risau W, Ruco L, Mantovani A, *et al.*: Monoclonal antibodies specific for endothelial cells of mouse blood vessels. Their application in the identification of adult and embryonic endothelium. *Eur J Cell Biol* 63: 247–254, 1994
41. Skalli O, Ropraz P, Trzeciak A, Benzonana G, Gillessen D, Gabbiani G: A monoclonal antibody against alpha-smooth muscle actin: A new probe for smooth muscle differentiation. *J Cell Biol* 103: 2787–2796, 1986
42. Kubbutat MH, Key G, Duchrow M, Schluter C, Flad HD, Gerdes J: Epitope analysis of antibodies recognising the cell proliferation associated nuclear antigen previously defined by the antibody Ki-67 (Ki-67 protein). *J Clin Pathol* 47: 524–528, 1994
43. LaRochelle WJ, Robbins KC, Aaronson SA: Immunochemical localization of the epitope for a monoclonal antibody that neutralizes human platelet-derived growth factor mitogenic activity. *Mol Cell Biol* 9: 3538–3542, 1989
44. Hu Y, Schett G, Zou Y, Dietrich H, Xu Q: Abundance of platelet-derived growth factors (PDGFs), PDGF receptors and activation of mitogen-activated protein kinases in brain decline with age. *Brain Res Mol Brain Res* 53: 252–259, 1998
45. Hu Y, Zou Y, Dietrich H, Wick G, Xu Q: Inhibition of neointima hyperplasia of mouse vein grafts by locally applied suramin. *Circulation* 100: 861–868, 1999
46. Matsumoto K, Hiraiwa N, Yoshiki A, Ohnishi M, Kusakabe M: PDGF receptor-alpha deficiency in glomerular mesangial cells of tenascin-C knockout mice. *Biochem Biophys Res Commun* 290: 1220–1227, 2002
47. Hirsch S, Gordon S: Polymorphic expression of a neutrophil differentiation antigen revealed by monoclonal antibody 7/4. *Immunogenetics* 18: 229–239, 1983
48. Alpers CE, Hudkins KL, Ferguson M, Johnson RJ, Rutledge JC: Platelet-derived growth factor A-chain expression in developing and mature human kidneys and in Wilms' tumor. *Kidney Int* 48: 146–154, 1995
49. Nakagawa H, Sasahara M, Haneda M, Koya D, Hazama F, Kikkawa R: Immunohistochemical characterization of glomerular PDGF B-chain and PDGF beta-receptor expression in diabetic rats. *Diabetes Res Clin Pract* 48: 87–98, 2000